We are IntechOpen, the world's leading publisher of Open Access books Built by scientists, for scientists

4,800
Open access books available

122,000
International authors and editors

135M
Downloads

Our authors are among the

154
Countries delivered to

TOP 1%
most cited scientists

12.2%
Contributors from top 500 universities

WEB OF SCIENCE™

Selection of our books indexed in the Book Citation Index in Web of Science™ Core Collection (BKCI)

Interested in publishing with us?
Contact book.department@intechopen.com

Numbers displayed above are based on latest data collected.
For more information visit www.intechopen.com

Chapter 4

Quantum Mechanical Approaches for Piezoelectricity Study in Perovskites

Edilson Luiz C. de Aquino,
Marcos Antonio B. dos Santos,
Márcio de Souza Farias, Sady S. da Silva Alves,
Fábio dos Santos Gil,
Antonio Florêncio de Figueiredo,
José Ribamar B. Lobato,
Raimundo Dirceu de P. Ferreira, Oswaldo Treu-Filho,
Rogério Toshiaki Kondo and José Ciríaco Pinheiro

Additional information is available at the end of the chapter

http://dx.doi.org/10.5772/62696

Abstract

In this chapter, we show the procedures we have been used to theoretically investigate the piezoelectric effects in perovskites. The construction of extended basis sets using the generator coordinate Hartree-Fock (GCHF) method is shown, as well as the strategies used to contract extended basis sets and to evaluate their quality in molecular calculations. Besides, we show adequate procedures to choice polarization and diffuse functions to best represent the studied crystal. In addition, we also discuss conditions under which GCHF basis sets and standard basis sets from literature can be used to theoretical investigation of piezoelectricity in perovskites. We finalize the chapter presenting and discussing the results for investigations of piezoelectricity with standard basis sets for barium and lanthanum titanates. To conclude, we present evidences that $BaTiO_3$ and $LaTiO_3$ may have piezoelectric properties caused by electrostatic interactions.

Keywords: basis sets, theoretical methods, quantum mechanical approaches, piezoelectricity, perovskites

1. Introduction

The worldwide growing demand for energy has led to increasing dependence on fossil fuels from few and unstable regions of the globe. Oppositely, clamors for more restrictive environmental regulation have pointed out the development of cleaner power supplies that meet the increasing demand for electricity.

The use of natural gas or their liquid fuels, the first and second generation of biofuel, and, even, hydrogen has been pointed as "clean" power supplies for the growing demand. Other classic solutions cover hydropower, solar, wind, and nuclear supplies which have enforcement power and limitations described by literature.

Piezoelectricity is a good alternative for clean and environmental power supply. It does not generate waste or pollutants because it does not need fuels or additives. Some revolutionary applications of this type of energy can be enumerated: piezoelectric plates in shoe soles can generate energy for charging portable electronic devices; piezoelectric plates in floors can be an alternative for lighting squares or dance clubs; and, even in a futuristic vision, piezoelectric materials can be used in pavements of highways or streets to generate inexpensive energy. This type of power supply can bring benefits to society and to environment because it can be obtained sustainably and be capable to replace other power supplies.

The piezoelectric effects were discovered in 1880 by brothers Pierre and Jacques Currie in quartz crystals. Ever since, piezoelectricity has been leading numerous researches in development of electronic transducer systems. The effect consists basically in conversion of mechanical energy to electrical energy (from Greek term "piezo" for pressure). In 1881, Lippman, using the thermodynamic analysis, predicted the existence of inverse piezoelectric effect, which consists in appearance of material deformation submitted to an electric field.

Two conditions must be presented simultaneously in a crystal to have piezoelectric property. First, it is the presence of uncentersymmetric characteristic in the crystalline structure of the material. Second, it is the existence of a material polarization when submitted under mechanical stress.

The piezoelectric effect is a reversible process for materials which present direct (internal generation of electric charge resulting from applied mechanical stress) and reverse (internal generation of mechanical stress resulting from applied electric field) effects. For example, lead zirconate titanate crystals generate measurable piezoelectricity when static structure is deformed by 0.1% from initial dimension. Oppositely, these same crystals change 0.1% of their static dimensions submitted to an external electric field.

Oxides as perovskites have a general formula ABO_3, where A is a large cation-like alkaline metals, earth metals, and rare earth metals and B is a small cation-like transition metals. Most common perovskites are those where A is a cation of rare earth metal with oxidation state +3 and B is a transition metal with the same valence state [1].

The perovskite structure is the most important piezoelectric crystalline ceramic. This structure is a network of cornered linked oxygen octahedral holes with a large cation filling the dodec-

http://dx.doi.org/10.5772/62696

ahedral holes. The piezoelectric properties in perovskite structure result from uncentersymmetric characteristic, since this physical property is originated from crystal anisotropy.

The first perovskite structure developed was barium titanate ($BaTiO_3$). The polymorphous forms of $BaTiO_3$ have been likened displacing the central Ti^{+4} ion within its oxygen octahedron toward one, two, and, then, three of the six adjacent oxygen ions as the temperature is lowered. This is a simplification of the actual atomic displacements, but it is a useful first approximation for structure understanding. For a revision about the role of the perovskite structure in ceramic science and technology, see literature [2].

The pragmatic application of theory in science follows two strategies: (i) there is readiness of experimental information of the interested system's properties (the application's results for the theory in study of those properties can be confronted to experimental data which will serve as guide to corroborate the applied concepts or to suggest changes) and (ii) experimental data are not available (the resulting forecasts of the application of theory can be used by experimentalists as guide to facilitate the rational money application and the time reduction for the system under investigation).

In last decade, we have been reported in literature a series of articles about theoretical studies of perovskites. Basically, our purpose is to investigate the possible existence of piezoelectric properties in those materials, using developed basis sets for the appropriate environment of their crystals. In our approaches, different theoretical methods have been used and the results suggest or not this property.

In this chapter, we show that the strategies have been used to study piezoelectricity in ceramic materials as perovskites using basis sets obtained by our research group. To obtain extended basis sets, we will show computer details using generator coordinate Hartree-Fock (GCHF) method [3] and the procedures used to contract extended basis sets as well as the strategy used to evaluate their quality in molecular environment. In addition, we will show the supplement of polarization and diffuse functions to best represent the studied crystal environment and the theoretical methods used in our articles in literature. We will also discuss conditions how our obtained basis sets and standard basis sets from packages in literature can be used to develop studies of piezoelectricity in perovskites.

Finally, we will present and discuss the obtained results for investigation of piezoelectricity with standard basis sets for barium and lanthanum titanates and last considerations related to this chapter.

2. The generator coordinate Hartree-Fock method and the construction of basis sets

In this section, we provide a brief history of the scientific scene that gave rise to the GCHF method and the atmosphere in which it has developed. We will also make a presentation of the GCHF method as strategy for building extended and contracted basis sets as well as the

procedure used to evaluate their quality and the selection of polarization and diffuse functions used in calculations of perovskites.

2.1. Brief history of scientific scene and atmosphere for the development of GCHF method

In 1957, the generator coordinate (GC) method for the nuclear bound state [4] was introduced in literature. According to this method, the variational trial function is written as an integral transform over a nucleonic wave function and a weight function depending on a parameter (GC), i.e., $f(\alpha)$. In this way, the common variational principle, $\delta E/\delta\alpha=0$ (where E is the total energy of system and α is the GC), a priori, was made more powerful with the requirement $\delta E/\delta f\alpha$, leading to an integral equation. Most applications in nuclear physics relied on the Gaussian overlap approximation (GOA). Although there were some attempts in numerical solution [5], the discussion of the GC method against the background of the Fredholm theory of linear integral equations was reported in literature [6, 7]. Probably the first application of GC to electrons in a molecular system (hydrogen molecule) was reported in literature in the second half of the 1970s [8]. After, the GC method was applied to several model problems, including the He atom, with special emphasis on various aspects of the discretization technique [9]. Besides, further developments in discretization techniques were reported in literature [10, 11].

On the other hand, in the late 1960s, the integral method for atomic and molecular systems was introduced in the literature, closely related to GC [12, 13]. In these applications, explicit forms were chosen for $f(\alpha)$ (as the delta function) leading to a variational treatment for the integration limits. Extensive bibliography on this method was found in literature [14].

The GCHF method was introduced in 1986 [3], and one of the first applications was in the generation of Gaussian- and Slater-type orbitals (GTO and STO) universal basis sets [15–17]. The GCHF method was used to build contracted GTF (Gaussian Type-Function) basis sets for the first- and second-row atoms which were applied in calculations of various properties at the HF, CISD (configuration interaction with single and double excitations), and MP2 (Möller-Plesset perturbation theory to second order) levels for a group of neutral and charged diatomic species [18, 19]. Also in the 1990s, efforts were concentrated on the development of GCHF formalism for molecular systems and the first applications have been focused on building basis for H_2, N_2, and Li_2 [20] and LiH, CO, and BF [21]. Applying GCHF basis sets for calculation of properties of polyatomic systems with the first application being concerned with the study of electronic properties and IR spectrum of high tridymite began in the second half of the 1990s [22]. First-principles (ab initio) calculations of electron affinities of enolates were also performed [23]. Theoretical interpretation of IR spectrum of hexaaquachromium (III) ion, tetraoxochromium (IV) ion, and tetraoxochromium (VI) ion [24] and theoretical interpretation of the Raman spectrum [25] and the vibrational structure of hexaaquaaluminum (III) ion [26] were also conducted with GCHF basis. Process of adsorption of sulfur on platinum (2 0 0) surface [27], infrared spectrum of isonicotinamide [28], and transition metal complexes [29–32] were also studied with GCHF basis sets.

http://dx.doi.org/10.5772/62696

2.2. Construction of extended and contracted basis sets for calculations in perovskites

The GCHF approach is based in choosing the one-electron functions as the continuous superposition:

$$\varphi_i(1)=\int \psi_i(1,\alpha) f_i(\alpha)\ d\alpha\ i=1,2,3,....n \tag{1}$$

where ψ_i are the generator functions (GTOs for the case of perovskites) and f_i are the weight functions (WFs) and ü is the GC.

The φ_i are then employed to build a Slater determinant for the multi-electronic wave function and minimizing the total energy with respect to $f_i(\alpha)$, which arrives to the HF-Griffin-Wheeler (HFGW) equations:

$$\int [F(\alpha,\beta) - \varepsilon_i S(\alpha,\beta)] f_i(\beta) d\beta = 0 \quad i = 1, 2, 3, \ldots\ldots\ldots m \tag{2}$$

where $ü_i$ are the HF eigenvalues and the Fock kernels, $F(\alpha,\beta)$ and $S(\alpha,\beta)$ are defined in Refs. [3, 16].

The HFGW equations are integrated numerically through discretization with a technique that preserves the integral character of the GCHF method, i.e., integral discretization (ID). The ID technique is implemented with a relabeling of the GC space [15], i.e.,

$$\Omega = \ln \alpha/A \qquad A > 1 \tag{3}$$

with A is a scaling parameter numerically determined. For perovskites $A = 6.0$.

The new GC Ω space is discretized, by symmetry, in an equally space mesh formed by ü values so that

$$\Omega = \Omega_{min} + (k+1)\Delta\Omega \quad k = 1,2,3,.....N \tag{4}$$

In Eq. (4), N corresponds to the number of discretization points defining the basis set size, Ω_{min} is the initial point, and ΔΩ is the increment.

The values of Ω_{min} (lowest value) and the highest value $\Omega_{max}=\Omega_{min}+(N-1)\Delta\Omega$ are chosen in order to adequately encompass the integration range of $f(\Omega)$. This is visualized by drawing the WFs from preliminary calculations with arbitrary discretization parameters. To illustrate the application of the GCHF method in the choice of basis sets for perovskites, we refer to our publication that investigates the piezoelectricity in $LaFeO_3$ [33]. **Figure 1** shows the respective 2s, 3p, and 5d weight functions for O (^{3}P), Fe (^{5}F), and La (^{2}D) atoms.

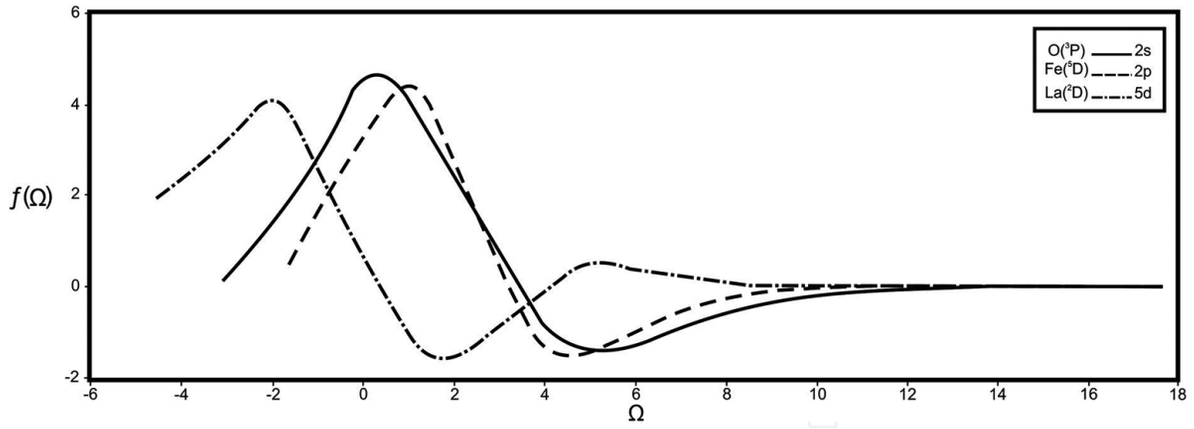

Figure 1. 2s, 3p, and 5d WFs for O (^{3}P), Fe (^{5}D), and La (^{2}D) atoms obtained with (20s14p), (30s19p13d), and (31s23p18d0 Gaussian) basis sets, respectively. Reproduction authorized by authors [33].

In the solution of the discretization of Eq. (2), the (22s14p), (30s19p13d), and (32s24p117d) GTOs basis sets were used to O (^{3}P), Fe (^{5}D), and La (^{2}D) atoms, respectively, as defined by the mesh of Eq. (3). The values of Ω_{min} and Ω_{max} were selected in order to satisfy the relevant integration range of each WF atom. In **Table 1**, the discretization parameters (which define the exponents) for the built basis sets are shown.

Symmetry	O			Fe			La		
	Ωmin	**ΔΩ**	***N***	**Ωmin**	**ΔΩ**	***N***	**Ωmin**	**ΔΩ**	***N***
s	−0.3969	0.122	22	−0.5998	0.114	30	−0.6304	0.115	32
p	−0.4387	0.119	14	−0.2758	0.110	19	−0.3938	0.104	24
d	–	–	–	−0.3771	0.117	13	−0.4532	0.113	17

[a]The scaling parameter used for s, p, and d symmetries for all atoms studied is equal to A = 6.0. Reproduction authorized by authors [33].

Table 1. Discretization parameters (which define the exponents) for O (^{3}P), Fe(^{5}D), and La(^{2}D) atoms[a].

For perovskite calculations, a basis set is usually developed in three stages: (1) construction of the extended basis set in atomic calculations, (2) construction of the contracted basis set using a segmented or general scheme (at this stage, due to increased availability of software access, we use the segmented contraction scheme), and (3) addition of supplementary functions of diffuse and polarization character. The first stage is usually a straightforward task. To illustrate the second step, we consider the segmented contraction [31] of basis sets to O (^{3}F), Fe (^{5}D), and La (^{2}D) atoms in $LaFeO_3$ [33]. The 20s14p basis set to O atom was contracted to 7s6p as follows: 16, 1, 1, 1, 1/9, 1, 1, 1. For Fe atom, the 30s19p13d GTO basis set was contracted to 13s8p6d according to 14, 3, 2, 2, 1, 1, 1, 1, 1, 1, 1/12, 1, 1, 1, 1, 1, 1, 1/8, 1, 1, 1, 1, 1. For La atom, the 32s24p17d GTO basis set was contracted according to 13, 2, 1, 1, 1, 1, 2, 1, 1, 1, 1, 1, 1, 1, 1, 1, 1/10, 2, 1, 1, 1, 1, 1, 2, 1, 1, 1, 1, 1/10, 2, 1, 1, 1, 1, 1.

2.3. Quality evaluation of the basis sets in perovskite calculations

In order to evaluate the quality of the contracted GTO basis sets in perovskite studies, the calculations of total energy, the highest occupied molecular orbital (HOMO) energy and the one level below to highest occupied molecular orbital (HOMO-1) energies for perovskites fragments at the HF level [35], are performed and the results are compared with those obtained from the extended GTOs basis sets. For $LaFeO_3$, the $^2FeO^{+1}$ and $^1LaO^{+1}$ fragments were studied. Comparison of the calculated values with the contracted and extended GTOs basis sets, respectively, shows differences of 0.2534 and 0.2827 hartree for the total energy and 8.8×10^{-4} and 1.26×10^{-3} hartree for the energy orbital. These values show a very good quality of the contracted GTOs basis sets for the study of properties of perovskite $LaFeO_3$ [33].

2.4. Supplementation of the basis sets with polarization and diffuse functions for calculations in perovskites

In order to better describe the properties of perovskite systems in the implementation of ab initio calculations, the inclusion of polarization functions in GTO basis sets is necessary. A methodology that has been a good strategy in the choice of polarization function for contracted GTOs bases sets is to extract the polarization function from the own Gaussian primitive basis set using successive calculations for the $[ABO_3]_2$ fragment for different primitive functions, taking into account the minimum energy criterion. For the $[LaFeO_3]_2$ fragment, the polarization function was included in the contracted GTO basis set for the O atom, i.e., $\alpha_d = 0.30029$ [33].

The role of the basis set is a crucial point in ab initio calculations of systems containing transition metals, since the description of the metal atom's configuration in complex is different from neutral state. In our studies with perovskites, the adequate diffuse functions for supplementation of contracted GTOs basis sets have been selected via one of the following methods: (1) the exponents of the basis sets are ranked according to magnitude and plotted on a logarithmic scale with equally spaced abscissas. Then the extrapolation of curve was done to smaller values of exponents, thereby obtaining exponents for a diffuse function [36] and (2) using the total energy optimization of the ground-state anions of the metals present in perovskite structure [37].

For $LaFeO_3$, the adequate diffuse functions were chosen using the first methodology described, i.e., for the contracted GTO basis set of Fe and La atoms, the diffuse functions are, respectively, $\alpha_s = 0.0138038$, $\alpha_p = 0.1000000$, and $\alpha_d = 0.054954$; $\alpha_s = 0.0125892$, $\alpha_p = 0.0446683$, and $\alpha_d = 0.0112201$.

The results obtained in the study of the perovskite $LaFeO_3$ with contracted GTO basis sets constructed with GCHF method strategy are well documented in literature [33].

3. Revision of basis sets and theoretical methods used to study the piezoelectric effect in perovskites

The literature reports different methods and basis sets built by GCHF method for investigation of perovskites' piezoelectric effects. The RHF (Restricted Hartree-Fock) method together with the 17s11p7d/11s6p6d/5s3p1d GTOs basis was used for investigation of perovskites' piezoelectricity of lanthanum manganite [38]. Besides, the ROHF (Restricted Open-shell Hartree-Fock) method and the 14s7p7d/11s7p7d/9s7p1d GTOs basis set allowed the calculations of electronic structure of yttrium manganite [39]. After, studies of piezoelectric effects were done in praseodymium manganite using ROHF method and 18s12p5d3f/9s6p4d/9s5p1d GTOs basis set [40], in $BaTiO_3$ using HF/16s9p5d/10s5p4d/6s4p1d GTOs method/basis set [41], as well as in lanthanum ferrite using HF/19s14p8d/14s9p7d/7s6p1d GTOs approximation/basis set [33]. Calculations for theoretical investigation of piezoelectric effect in samarium titanate and in yttrium ferrite were developed using DKH level (Douglas-Kroll-Hess second-order scalar relativistic) with 17s12p8d4f/10s6p3d/5s4p1d GTOs [42] and 14s9p8d/14s8p6d/6s4p1d [37] basis sets, respectively. On the other hand, quantum chemical studies for piezoelectricity of yttrium titanate and gadolinium niquelate using DKH approximation were been reported in literature. For the yttrium titanate, the 16s10p7d/11s6p5d/6s5p1d GTOs basis set was used [43], while, for gadolinium niquelate, the used basis set was 20s14p10d6f/13s8p7d/6s4p1d GTOs [44].

In the developed studies for piezoelectricity investigation, standard basis sets from literature mostly showed inefficient for theoretical description of studied perovskites, and, therefore, the electronic structure description of these materials is inadequate for a satisfactory interpretation of this effect. For this reason, we recommend the use of GCHF method strategy; even standard basis sets are inappropriate to describe the geometric parameters of studied perovskites under the piezoelectric effect perspective. Furthermore, using GCHF method basis sets allows choosing the ideal basis set to better describe the studied polyatomic environment.

4. Investigation of piezoelectricity in perovskites using standard basis sets in barium titanate ($BaTiO_3$) and lanthanum titanate ($LaTiO_3$)

In this section, we investigate the piezoelectricity in $BaTiO_3$ and $LaTiO_3$ perovskites. Initially, we apply the methodology for the $BaTiO_3$ to verify if the results show the piezoelectricity property, once it is known this perovskite has it. After, we apply the same methodology for $LaTiO_3$ and the results are analyzed to check the property. **Figure 2** shows crystallographic units of studied perovskites.

4.1. Computational

The calculations were done using the basis set of Lan2DZ (Los Alamos National Laboratory dupla zeta) [45–47] at the density functional theory (DFT) level. In the DFT calculations, we

http://dx.doi.org/10.5772/62696

have employed the Becke's 1988 functional [48] using the LYP (Lee-Yang-Parr) correlation functional [49] as implemented in the Gaussian 98 program [50].

For the study of the crystalline 3D periodic $BaTiO_3$ [51] and $LaTiO_3$ [52] systems (**Figure 2**), it is necessary to choose a fragment (or a molecular model), which represents adequately a physical property of the crystalline system as a whole.

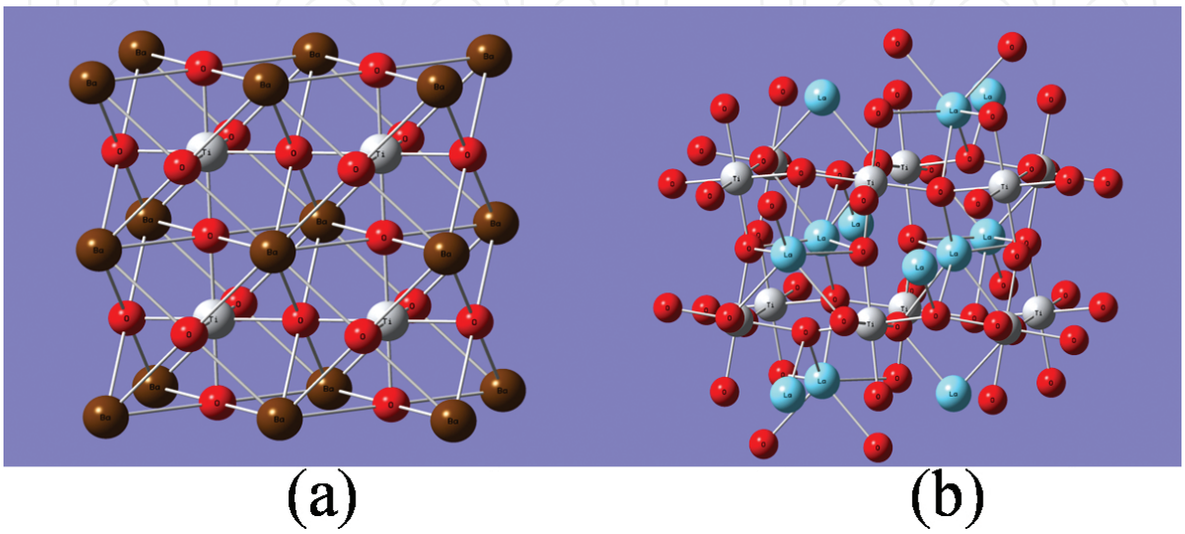

Figure 2. Crystallographic units $BaTiO_3$ (a), features seen, O atoms (red), Ti atoms (white), and Ba atoms (brown) and $LaTiO_3$ (b), features seen, O atoms (red), Ti atoms (white), and La atoms (blue), from which the fragments were extracted for study.

Figure 3 shows the molecular models used to simulate the necessary conditions of the existence of piezoelectricity in $BaTiO_3$ [51] and $LaTiO_3$ [52] as full solids. The $[BaTiO_3]_2$ and $[LaTiO_3]$ fragments were chosen because, after its optimization, the obtained structural parameters (interatomic distances) were close to experimental values with very good precision. For the two systems, the Ti is located in the center of the octahedron being wrapped up for six O atoms, disposed in the reticular plane (2 0 0), and two Ba or La atoms arranged in the reticular plane (1 0 0).

In this study, the following strategy was used: (i) initially, it was made the geometry optimization of the $[BaTiO_3]_2$ and $[LaTiO_3]_2$ fragments in the C_s symmetry and 1A' electronic state; (ii) at last, with the geometry optimized according to the descriptions presented in **Figure 3**, single-point calculations were developed.

In **Figure 3**, (a) represents the $[BaTiO_3]_2$ fragment with the Ti atom fixed in the space and Ti atom being moved 0.003 Å in the direction to O_1, O_2, O_3, O_4, O_5, and O_6 atoms and Ba atom and all O atoms are fixed; (b) represents the $[BaTiO_3]_2$ fragment with the bond lengths Ti—O_1, Ti—O_6 shortened from 0.003 Å; (c) represents the $[LaTiO_3]_2$ fragment with the Ti atom fixed in the space and Ti atom being moved 0.005 Å in the direction to O_1, O_2, O_3, O_4, O_5, and O_6 atoms and La atom and all O atoms are fixed; and (d) represents the $[LaTiO_3]_2$ fragment with the bond lengths Ti—O_1, Ti—O_6 shortened from 0.005 Å.

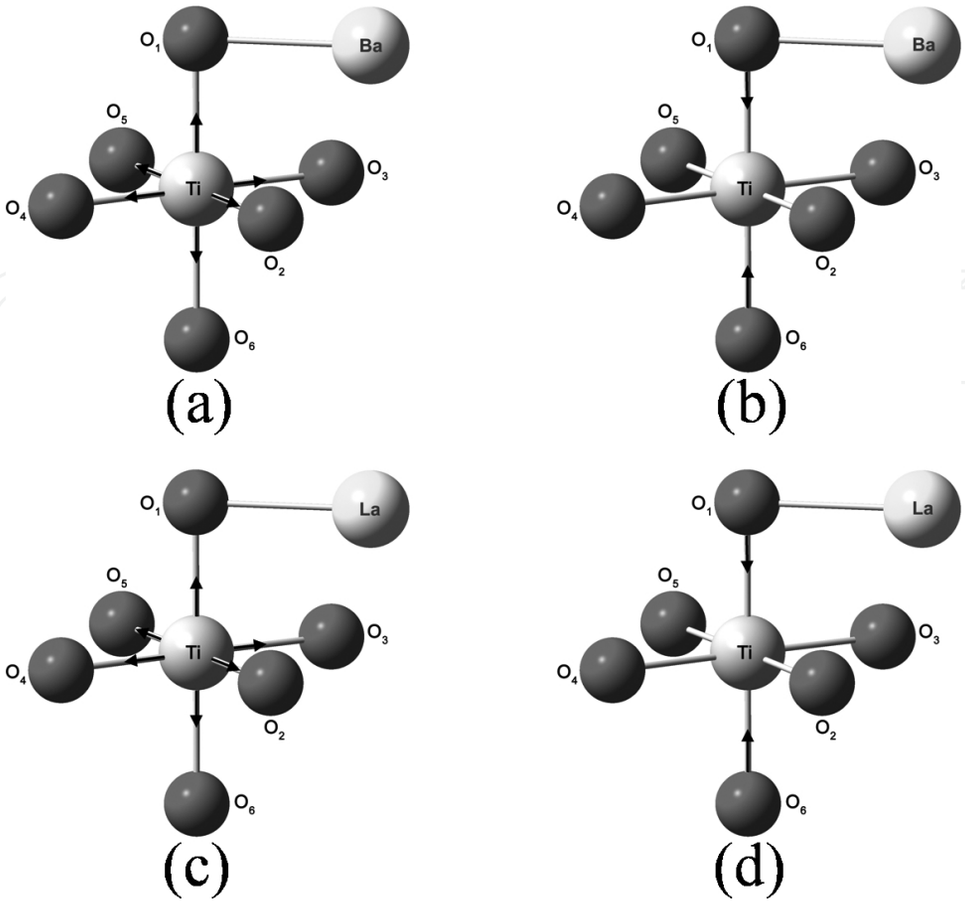

Figure 3. (a) represents the $[BaTiO_3]_2$ fragment with the Ti atom fixed in the space and Ti atom being moved 0.003 Å in the direction to O_1, O_2, O_3, O_4, O_5, and O_6 atoms and Ba atom and all O atoms are fixed; (b) represents the $[BaTiO_3]_2$ fragment with the bond lengths Ti—O_1 and Ti—O_6 shortened from 0.003 Å; (c) represents the $[LaTiO_3]_2$ fragment with the Ti atom fixed in the space and Ti atom being moved 0.003 Å in the direction to O_1, O_2, O_3, O_4, O_5, and O_6 atoms and La atom and all O atoms are fixed; and (d) represents the $[LaTiO_3]_2$ fragment with the bond lengths Ti—O_1 and Ti—O_6 shortened from 0.003 Å.

4.2. Results and discussion

Table 2 shows the theoretical (calculated) bond lengths and the experimental values from literature [51] for $BaTiO_3$. The theoretical values are closer to the experimental data. The deviations between the theoretical and literature values are 6.32×10^{-2} and 6.39×10^{-2} Å for Ti—O_1 and Ba—O_1, respectively.

Bond length (Å)	Theoretical (this work)	Experimental [51]	Δ
T_i—O_1	1.93431	1.99750	6.32×10^{-2}
Ba—O_1	2.77480	2.83871	6.39×10^{-2}

Δ = |Theoretical − experimental|

Table 2. Experimental and theoretical geometric parameters obtained for $BaTiO_3$ by $[BaTiO_3]_2$ fragment optimization.

http://dx.doi.org/10.5772/62696

Table 3 presents the total energy of $[BaTiO_3]_2$ fragment. As it mentioned previously, the calculations are at atomic positions: Ti is fixed in space, Ti is moved toward the O_1 atom and Ba atom and the O other atoms are fixed, Ti is moved toward the O_2 atom and Ba atom and the O other atoms are fixed, and so on. The results in **Table 3** show that when the Ti atom is displaced relative to the fixed position, the fragment is 4.32×10^{5}, 8.20×10^{-5}, 1.08×10^{-4}, 8.38×10^{-4} , 8.54×10^{-4}, 7.39×10^{-4} hartree more stable, indicating the Ti^{+4} central ion is not centersymmetric. Also we can see that decreasing the Ti—O_1 and Ti—O_6 bond lengths (mechanical stress), the energy calculation shows less stable fragment compared to the system without mechanical stress (Ti fixed in space).

Ti atom position	**TE (hartree)**
Ti is fixed in space	−534.259022802
Ti is moved toward the O_1 atom; Ba and O atoms are fixed	−534.259066114
Ti is moved toward the O_2 atom; Ba and O atoms are fixed	−534.259104826
Ti is moved toward the O_3 atom; Ba and O atoms are fixed	−534.259130429
Ti is moved toward the O_4 atom; Ba and O atoms are fixed	−534.259860527
Ti is moved toward the O_5 atom; Ba and O atoms are fixed	−534.259877355
Ti is moved toward the O_6 atom; Ba and O atoms are fixed	−534.259762234
Bond lengths Ti—O_1 and Ti—O_6 are shortened (mechanical stress)	−534.257326207

Table 3. Total energy of $[BaTiO_3]_2$ fragment.

	Ti atom position	
Atom	**Ti is fixed in space**	**Bond lengths Ti—O_1 and Ti—O_6 are shortened (mechanical stress)**
Ti	+0.885	+0.887
Ba	+1.837	+1.841
O_1	−0.636	−0.633
O_2	−0.564	−0.563
O_3	−0.664	−0.663
O_4	−0.291	−0.295
O_5	−0.296	−0.300
O_6	−0.271	−0.274
Dipole moment (Debye)		
μ_x	23.28	−23.51
μ_y	−0.3622	0.1374
μ_z	−2.0703	0.0585
μ	23.38	23.51

Table 4. Total atomic charges and dipole moment of the $[BaTiO_3]_2$ fragment.

Table 4 shows the values of the total charges of the atoms for Ti atom fixed in space and for the fragment under the influence of mechanical stress and the dipole moments, respectively. Also, it shows the rearrangement of the charges in all atoms caused by a mechanical stress comparing with the Ti position fixed in space. As well as we can notice the change in the dipole moment resulting from this mechanical stress. The rearrangement of the charges and the variation of the dipole moment can lead us to suppose that the decrease of Ti—O_1 and Ti—O_6 chemical bond lengths provokes a polarization of the $[BaTiO_3]_2$ fragment, indicating the nature of Ti—O and Ba—O chemical bonds was changed.

For the $[BaTiO_3]_2$ fragment with Ti atom fixed in space, the HOMO (Highest Occupied Molecular Orbital) and the LUMO (Lowest Unoccupied Molecular Orbital)are represented, respectively, by

$$\text{HOMO} = 0.63\left(2p_z\right)O(1) - 0.46\left(2p_z\right)O(2) + 0.15\left(2p_z\right)O(3) + 0.16\left(2p_z\right) O(4) + 0.57\left(2p_z\right)O(5) - 0.21\left(2p_z\right)O(6)$$

$$\text{LUMO} = +0.17\left(2p_x\right)O(1) + 0.33\left(2p_y\right)O(1) + 0.12\left(2p_z\right)O(1) + 0.42\left(2p_x\right)O(2) + 0.41\left(2p_x\right) O(3) + 0.34\left(2px\right)O(4) + 0.36\left(2p_x\right)O(5) + 0.56\left(2p_x\right)O(6)$$

For the fragment $[BaTiO_3]_2$ under mechanical stress, the HOMO and the LUMO are written as

$$\text{HOMO} = +0.64\left(2p_y\right)O(1) - 0.44\left(2p_z\right)O(2) + 0.35\,2p_zO(3) - 0.12\left(2p_z\right)O(3) + 0.18\left(2p_y\right) O(4) - 0.35\left(2p_z\right)O(4) + 0.16\left(2p_y\right)O(5) + 0.44\left(2p_z\right)O(5) - 0.34\left(2p_y\right)O(6)$$

$$\text{LUMO} = +0.18\left(2p_x\right)O(1) - 0.31\left(2p_z\right)O(1) + 0.41\left(2p_x\right)O(2) + 0.42\left(2p_x\right) O(3) + 0.38\left(2p_x\right)O(5) + 0.56\left(2p_x\right)O(6)$$

The analysis of the HOMO and the LUMO of the $[BaTiO_3]_2$ fragment shows the mechanical stress does not cause appearance of chemical bonds with contributions of barium atom's 4d orbitals. This fact together with the changing of the nature of Ti—O and Ba—O chemical bonds leads us to suggest that electrostatic interactions are very important in electronic structure of $[BaTiO_3]_2$ fragment. This is consistent because the repulsive effect of d electrons in both high-spin and low-spin octahedral species of ML complexes (M = Metal and L = Ligand), all d electron density will repel the bonding electron density [53]. This shows that the piezoelectricity in $BaTiO_3$ can be caused by electrostatic interactions.

The experimental [52] and theoretical geometric parameters for $LaTiO_3$ are shown in **Table 5**. According to **Table 5**, the theoretical results are 2.02413 and 2.58928 Å for Ti—O_1 and La—O_1,

respectively, while the experimental values are 2.01556 and 2.59918 Å. The differences between the theoretical and experimental values are 8.57×10^{-3} and 9.99×10^{-3} Å.

Bond length (Å)	Theoretical (this work)	Experimental [52]	Δ
T_i—O_1	2.02413	2.01556	8.57×10^{-3}
La—O_1	2.58928	2.59918	9.99×10^{-3}

Δ = |Theoretical − experimental|

Table 5. Experimental and theoretical geometric parameters obtained for $LaTiO_3$ by $[LaTiO_3]_2$ fragment optimization.

Table 6 presents the total energy from $[LaTiO_3]_2$ fragment. As mentioned previously, the calculations are at atomic positions: Ti is fixed in space, Ti is moved toward the O_1 atom and La atom and the O other atoms are fixed, Ti is moved toward the O_2 atom and La atom and the O other atoms are fixed, and so on. According to **Table 6**, the fragment is stable 8.16×10^{-2}, 3.36×10^{-2}, 5.70×10^{-2}, 7.04×10^{-2}, 1.72×10^{-2}, and 2.87×10^{-2} hartree to the titanium atom moving to the positions O_1, O_2, O_3, O_4, O_5, and O_6, respectively, when fixed in space. Also, for the $[LaTiO_3]_2$ fragment, we can note that, with the shortening of Ti—O_1 and Ti—O_6 chemical bonding (mechanical stress), the system becomes less stable.

Ti atom position	TE (hartree)
Ti is fixed in space	−540.247808392
Ti is moved toward the O_1 atom; La and O atoms are fixed	−540.329458501
Ti is moved toward the O_2 atom; La and O atoms are fixed	−540.281387651
Ti is moved toward the O_3 atom; La and O atoms are fixed	−540.304861376
Ti is moved toward the O_4 atom; La and O atoms are fixed	−540.318198767
Ti is moved toward the O_5 atom; La and O atoms are fixed	−540.265005660
Ti is moved toward the O_6 atom; La and O atoms are fixed	−540.276475167
Bond lengths Ti—O_1 and Ti—O_6 are shortened (mechanical stress)	−532.224697936

Table 6. Total energy of $[LaTiO_3]_2$ fragment.

Table 7 shows the total atomic charges and the dipole moment values for the $[LaTiO_3]_2$ when the Ti atom is fixed in space and under mechanical stress. In **Table 7**, we can see, when the Ti atom is fixed in space, the La atom presents positive charge as expected. However, with mechanical compression, the La atom receives electrons, presenting negative charge. It can be characterized by appearance of a pair of free electrons in its 5d orbitals. We can also notice a wide variation of charges in oxygen atoms. Therefore, as $BaTiO_3$, $LaTiO_3$ also presents piezoelectric property due to electrostatic effects with strong variation of the dipole moment as shown in **Table 7**.

	Ti atom position	
Atom	**Ti is fixed in space**	**Bond lengths Ti—O_1 and Ti—O_6 are shortened (mechanical stress)**
Ti	+0.967	+2.229
La	+1.451	−0.212
O_1	−0.492	−0.691
O_2	−0.010	+4.16
O_3	−0.553	−0.527
O_4	−0.267	−1.803
O_5	−0.297	−1.766
O_6	−0.799	−1.390
Dipole moment (Debye)		
μ_x	25.71	34.67
μ_y	2.806	40.92
μ_z	0.716	25.24
μ	25.87	59.29

Table 7. Total atomic charges and dipole moment of the $[LaTiO_3]_2$ fragment.

For the $LaTiO_3$, the HOMO and the LUMO, when the Ti atom is fixed in space, are, respectively,

$$\begin{aligned}\text{HOMO} = &+0.10\,2p_zO(3)+0.21\,2p_xO(4)+0.42\,2p_yO(4)+0.14\,2p_zO(4)+0.11\,2p_xO(5)\\&+0.60\,2p_yO(5)+0.39\,2p_yO(6)-0.34\,2p_xO(6)\end{aligned}$$

$$\begin{aligned}\text{LUMO} = &+0.14\,2p_xO(2)-0.38\,2p_yO(2)-0.13\,2p_zO(3)+0.20\,2p_xO(4)-0.18\,2p_yO(4)\\&+0.62\,2p_zO(4)-0.15\,2p_xO(5)+0.15\,2p_yO(5)+0.53\,2p_zO(5)-0.14\,2p_yO9(6)\end{aligned}$$

For the $LaTiO_3$ fragment under mechanical stress, the HOMO and the LUMO are

$$\begin{aligned}\text{HOMO} = &+0.78(6s)\,\text{La}+0.35(5p_x)\,\text{La}-0.12(5p_y)\,\text{La}-0.25(5d_z^2)\\&\text{La}-0.18(5d_{xz})\,\text{La}+0.41(5d_{yz})\,\text{La}-0.40(5d_{xy})\,\text{La}\end{aligned}$$

$$\begin{aligned}\text{LUMO} = &+0.37(2p_y)\,O(1)-0.27(6s)\,\text{La}-0.17(5p_x)\,\text{La}+0.12(5p_y)\\&\text{La}+0.83(5d_{yz})\,\text{La}+0.49(5d_{xz})\,\text{La}\end{aligned}$$

http://dx.doi.org/10.5772/62696

Analyzing the HOMO and the LUMO of $LaTiO_3$ fragment, with Ti atom fixed in space and under compression, we can notice that, initially, the system does not present contributions of 5d orbital of La atom for the HOMO and the LUMO. Nevertheless, the mechanical stress has led to the appearance of contributions of this orbital (5d) in the HOMO and the LUMO of the fragment. This confirms that these orbitals work as a pair of free electrons causing the appearance of negative charge in lanthanum atom as shown in **Table 7**.

5. Concluding remarks

We present a methodology we developed using the GCHF to build basis sets and to study piezoelectric effects in ceramic materials as perovskite. The GCHF method is a legitimate alternative for the standard basis sets available in packages for polyatomic system calculations. Even for cases where standard basis sets do not present computational problems, the GCHF method is still a good alternative due to the possibility of building basis sets from the own polyatomic system environment. Besides, the availability of basis sets built by GCHF method or other variant methodologies is rich documented in literature. Therefore, it is possible, having components of the atomic basis sets for perovskite systems, to apply portion of the presented methodology to obtain contracted basis sets with well-supplemented and representative polarization and diffuse functions to study piezoelectric properties of this type in ceramic material. We also demonstrated the use of different possibilities of theoretical approximations for calculation of these properties, which embrace approximations with more or less inclusion of electronic correlation energy as well as approximations with relativistic correction effect for better description of the studied property.

To conclude this chapter, we presented our strategy to investigate the piezoelectric effect of two perovskite (barium and lanthanum titanates) using standard basis set and the DFT. Thus, the presented methodology is a legitimate alternative to investigate theoretically piezoelectric properties in ceramic materials as perovskites.

Author details

Edilson Luiz C. de Aquino[1], Marcos Antonio B. dos Santos[1], Márcio de Souza Farias[1], Sady S. da Silva Alves[2], Fábio dos Santos Gil[1], Antonio Florêncio de Figueiredo[2], José Ribamar B. Lobato[1], Raimundo Dirceu de P. Ferreira[1], Oswaldo Treu-Filho[3], Rogério Toshiaki Kondo[4] and José Ciríaco Pinheiro[1*]

*Address all correspondence to: ciriaco@ufpa.br

1 Computational and Theoretical Chemistry Laboratory, Federal Institute of Education, Science and Technology, Pará, Brazil

2 Federal University of Pará, Pará, Brazil

3 Chemistry Institute, Araraquara, São Paulo, Brazil

4 Office of Information Technology, University of São Paulo, Brazil

References

[1] Müller KA, Kool TW, editors. Properties of Perovskites and Other Oxides. New Jersey: World Scientific; 2010. DOI: 10.1080/00107514.2912.657688

[2] Bhalla AS, Guo R, Roy R. The perovskite structure – a review of its role in ceramic science and technology. Materials Research Innovation. 2000;4:3–26. ISSN: 1432-8917.

[3] Mohallem JR, Dreizler RM, Trisc M. A Griffin Hill–Wheeler version of the Hartree–Fock Equations. International Quantum Chemistry: Quantum Chemistry Symposium. 1986;20:45–55. DOI: 10.1002/qua.560300707.

[4] Griffin JJ, Wheeler JA. Collective motions in nuclei by the method of generator coordinates. Physical Review. 1957;108:311–327. DOI: http://dx.do.org/10.1103/PhysRev.108.311.

[5] Justin JD, Mihailovic MV, Rosina M. A generator coordinate approach for the description of pairing vibrations in the seniority-zero space. Nuclear Physics A. 1972;182:54–68. ISSN: 0375-9474.

[6] Lathouwers L. The generator coordinate representation in a natural state formalism. Annals Physics. 1976;102:347–370. ISSN: 0003-4916.

[7] Lathouwers L, Van Lauven P, Bouten M. Quantum theory and molecular spectra. Chemical Physics Letters. 1977;52: 439–441. ISSN: 0009-2614.

[8] Laskowski B. Quantum Science Methods and Structure. A tribute to Per-Olov Löwdin, J. L. Calais; O. Goscinski; J. Linderberg and Y. Öhrn, editors. New York: Plenum; 1976

[9] Chattopadhyay P, Dreizler RM, Trsic M, Fink M. Illustration of the generator coordinate method in terms of model problems. Zietschrift für Physik A. 1978;285:7–16. ISSN: 0939-7922.

[10] Broeckhove J, Deumens E. A mathematical foundation for discretization techniques in the generator coordinate method. Zietschrift für Physik A. 1979;292:243–247. ISSN: 0939-7922.

[11] Arickx F, Broeckhove J, Deumens E, Van Leuven P. Variational discretization: a new algorithm for the generator coordinate method. Journal of Computational Physics. 1981;39:272–281. ISSN: 0021-9991.

[12] Somorjai RL. Integral transform functions. A new class of approximate wave functions. Chemical Physics Letters. 1968;2:339–401. ISSN: 0009-2614.

[13] Somorjai RL. Systematic construction of correlated many-particle integral-transform trial functions and multicenter molecular orbitals. Physical Review Letters. 1969;23:329–331. ISSN: 0031-9007.

[14] Bishop DM, Schneider BE. A new integral transform basis function. International Journal of Quantum Chemistry. 1975;9:67–74. DOI: 10.1002/qua.560090108

[15] Mohallem JR, Trisc M. A universal Gaussian basis sets for atoms Li through Ne based on a generator coordinate version of the Hartree–Fock equations. Journal of Chemical Physics. 1987;86:5043–5044. DOI: 10.1063/1.452680.

[16] Da Costa HFM, Trsic M, Mohllem JR. Universal Gaussian and Slater type basis-sets or atoms He to Ar based on integral version of the Hartree–Fock equations. Molecular Physics. 1987;62:91–95. ISSN: 0026-8976.

[17] Da Costa HFM, Mohallem JR, Trsic M. The weight functions for He to Ar Gaussian and Slater type universal basis sets originated by the integral Hartree–Fock method. Química Nova. 1988;11:41–58. ISSN: 0100-4042.

[18] Pinheiro JC, Da Silva ABF, Trsic M. The generator coordinate Hartree–Fock method Applied to choice of a contracted gaussian basis for first-row atoms. Journal of Molecular Structure (Theochem). 1997;394:107–115. ISSN: 0166-1280.

[19] Pinheiro JC, Da Silva ABF, Trsic M. Generator coordinate Hartree–Fock method applied to the choice of a contracted Gaussian basis for the second-row atoms. International Journal of Quantum Chemistry. 1997;63:927–934. DOI: 10.1002/(SICI)1097-461X(1997)63:5<927

[20] Da Costa HFM, Da Silva ABF, Mohallem JR, Simas AM, Trisc M. The generator coordinate Hartree–Fock method for molecular systems. Formalism and first applications to H_2, LiH and Li_2. Chemical Physics. 1991;154:379–384. ISSN: 0301-0104

[21] Da Costa HFM, Simas AM, Smith Jr VH, Trsic M. The generator Hartree–Fock method for molecular systems. Near Hartree–Fock limit calculations for N_2, CO and BF. Chemical Physics Letters. 1992;192:195–198. ISSN: 0009-2614.

[22] Jardim IN, Treu-Filho O, Martines MAU, Davolos MR, Jafelicci Jr M, Pinheiro JC. Ab initio study of high tridymite by the formalism generator coordinate Hartree–Fock. Journal of Molecular Structure (Theochem). 1999; 464:15–21. ISSN: 0166-1280.

[23] Savedra RML, Pinheiro JC, Teu-Filho O, Kondo RT. Gaussian basis sets by generator coordinate Hartree–Fock method to ab initio calculations of electron affinities of enolates. Journal of Molecular Structure (Theochem). 2002;587:9–17. ISSN: 0166-1280.

[24] Savedra RML, De Lima KCV, Pinheiro JC, Kondo RT, Treu-Filho O, Davolos MR, Jafelicci Jr. M, Martines MAU. Design of Gaussian basis sets to the theoretical interpretation of IR-spectrum of hexaaquachromium (III) ion, tetraoxochromium (IV) ion, and tetraoxochromium (VI) ion. Journal of Molecular Structure (Theochem). 2003;633:83–92. DOI: 10.1016/S0166-1280(03)00330-0.

[25] Treu-Flho O, Kondo RT, Pinheiro J.C.. Contracted GTF basis sets applied to the theoretical interpretation of the Raman spectrum of hexaaquachromium (III) ion. Journal od Molecular Structure (Theochem). 2003;624:153–157. ISSN: 0166-1280.

[26] Treu-Filho O, Pinheiro JC, Kondo RT. Basis sets applied to the theoretical study of the vibrational structure of hexaaquaaluminium (III) ion. Journal of Molecular Structure (Theochem). 2004;668:109–112. DOI: 10.1016/j.theochem.2003.10.030.

[27] Treu-Filho O, Pinheiro JC, Kondo RT. The generator coordinate Hartree–Fock method as strategy for building Gaussian basis sets to *ab initio* study of the process of adsorption of sulfur on platinum (2 0 0) surface. Journal of Molecular Structure (Theochem). 2005;716:89–92. DOI: 10.1016/j.theochem.2004.10.080

[28] Treu-Filho O, Pinheiro JC, Da Costa EB, Kondo RT, De Souza RA, Nogueira VM, Mauro AE. Theoretical and experimental study of the infrared spectrum of isonicotinamide. Journal of Molecular Structure (Theochem). 2006;763:175–179. DOI:10.1016/j.theochem.2005.08.046.

[29] Treu-Filho O, Pinheiro JC, De Souza RA, Kondo RT, Ferreira RDP, De Figueiredo AF, Mauro AE. Molecular structure and vibrational frequencies for *cis*-[$PdCl_2$(tmen)] and *cis*-[$Pd(N_3)_2$(tmen)]: a DFT study. Inorganic Chemistry Communications. 2007;10:1501–1504. DOI: 10.1016/j.inoche.2007.09.017.

[30] Treu-Filho O, Pinheiro JC, Da Costa EB, Ferreira JEV, De Figueiredo AF, Kondo RT, Lucca Neto VA, De Souza RA, Legendre AO, Mauro AE. Experimental and theoretical study of the compound [Pd(dmba)(NCO)(imz)]. Journal of Molecular Structure. 2007;829:195–201. DOI: 10.1016/j.molstruc.2006.06.018.

[31] Treu-Filho O, Rocha FV, Neto AVG, Pinheiro JC, Utuni VHS, Kondo RT, Mauro AE. Molecular structures and vibrational frequencies for [PdX_2(tdmPz)] (X = Cl—, SCN): a DFT study. Journal of Molecular Structure. 2009;921:239–243. DOI: 10.1016/j.molstruc.2008.12.066.

[32] Barra CV, Treu-Filho O, Rocha FV, Moura TR, Netto AVG, Mauro AE, Pinheiro JC, Kondo RT. Experimental and DFT Study on the Compounds [$PdCl_2L_2$] (L = 4-methylpyrazole, 4-iodopyrazole). Acta Chimica Slovenic. 2015;62:662–671. DOI: 10.17344/acs.2014.1299.

[33] Dos Santos CC, Barbosa JP, Dos Santos MAB, Lira FAM, Cardoso FJB, Pinheiro JC, Treu-Filho O, Kondo RT. Investigation of piezoelectricity in perovskite ($LAFeO_3$): a theoretical study. Computational Materials Science. 2007;39:713–717. DOI: 10.1016/j.commatsci.2006.09.004.

[34] Dunning Jr. TH, Hey PJ. Methods of Electronic Structure Theory. in: H. F. Schaefer III, editor. Plenum: New York, 1977. ISBN: 978-1-4757-0887-5.

[35] Roothaan CCJ. New developments in molecular orbital theory. Reviews of Modern Physics. 1951;23:69–88. ISSN: 0034-6861.

[36] Raffenetti RC. General contraction of Gaussian atomic orbitals: core, valence, polarization, and diffuse basis sets; molecular integral evaluation. Journal of Chemistry Physics. 1973;58:4452–4458. DOI: 10.1063/1.167.9007.

[37] De Lira FAM, Farias MS, De Figueiredo AF, Gil FS, Dos Santos MAB, Malheiros BV, Ferreira JEV, Pinheiro JC, Treu-Filho O, Kondo RT. Quantum chemical modeling of perovskite: an investigation of piezoelectricity in ferrite of yttrium. Journal of Molecular Modeling. 2011,17:1621–1624. DOI: 10.1007/s00894-010-0797-2.

[38] Treu-Filho O, Pinheiro JC, Kondo RT, Marques RFC, Paiva-Santos CO, Davolos MR, Jafelicci Jr. M. Gaussian basis sets to the theoretical study to the electronic structure of perovskite ($LaMnO_3$). Journal of Molecular Structure (Theochem). 2003;631: 93–99. DOI: 10.1016/S0166-1280(03) 00207-0.

[39] Treu-Filho O, Pinheiro JC, Kondo RT, Marques RFC, Paiva-Santos CO, Davolos MR, Jafelicci Jr. M. Development of basis sets to calculations of the electronic structure of $YMnO_3$. Journal of Molecular Structure (Theochem). 2003;629:21–26. DOI: 10.1016/S0166-1280(03)00004-6.

[40] Treu-Filho O, Pinheiro JC, Kondo RT, Jafelicci Jr. M. GCHF basis sets and their application in the electronic structure study of $PrMnO_3$. Journal of Molecular Structure (Theochem). 2004;668:113–117. DOI: 10.1016/j.theochem.2003.10.031.

[41] Treu-Filho O, Pinheiro JC, Kondo RT. Designing Gaussian basis sets to the theoretical study of the piezoelectricity effect of perovskite ($BaTiO_3$). Journal of Molecular Structure (Theochem). 2004;671:71–75. DOI: 10.1016/j.theochem.2003.10.032.

[42] Da Costa EB, Farias MS, De Miranda RM, Dos Santos MAB, Lobato MS, De Figueiredo AF, Ferreira RDP, Gil FS, Pinheiro JC, Treu-Filho O, Kondo RT. An insight into the theoretical investigation of possible piezoelectric effect in samarium titanate ($SmTiO_3$). Computational Material Sciences. 2009;44:1150–1152 DOI: 10.1016/j.commatsci.2008.07.028.

[43] Ferreira RDP, Dos Santos MAB, Lobato MS, Barbosa JP, Farias MS, De Figueiredo AF, Treu-Filho O, Kondo RT. Quantum mechanical study of $YTiO_3$ to the investigation of piezoelectricity. Physics Research International. 2011;Article ID 123492:5 pages. DOI: 10.1155/2011/123492.

[44] Dos Santos CC, Dos Santos MAB, Barbosa JP, Farias MS, Ferreira JV, Almeida RCO, Lobato MS, Pinheiro JC, Treu-Filho O, Kondo RT. Electronic structure of perovskite: an *ab initio* study of the piezoelectricity in $GdNiO_3$. Journal of Advanced Mathematics and Applications. 2014;2:139–146. DOI: 10.1166/jama.2014.1038.

[45] Hay PJ, Wadt WR. Ab initio effective core potentials for molecular calculations – potentials for the transition-metal atoms Sc to Hg. Journal of Chemical Physics. 1985;82:270–283. DOI: 10.1063/1.448799

[46] Wadt WR, Hay PJ. Ab initio effective core potentials for molecular calculations – potentials for main Group elements Na to Bi. Journal of Chemical Physics. 1985;82:284–298. DOI: 10.1063/1.448800.

[47] Hay PJ, Wadt WR. Ab initio effective core potentials for molecular calculations–potentials for K to Au including the outermost core orbitals. Journal of Chemical Physics. 1985;82:299–310. DOI: 10.1063/1.448975.

[48] Becke AD. Density-functional exchange-energy approximation with correct asymptotic behavior. Physical Review. 1988;38A:3098–3100. DOI: http://dx.doy.org/10.1103/RevA.38.3098.

[49] Lee C, Yang W, Parr RG. Development of the Colle–Salvetti correlation-energy formula into a functional of the electron density. Physical Review. 1988;B37:785–789. ISSN: 2469-9950.

[50] Fisch MJ, Trucks GW, Schlegel HB, Gill PMW, Johnson BG, Robb MA, Cheeseman JR, Keith TA, Peterson GA, Montgomerey JA, Raghavachari K, Al-Laham MA, Zkrzewski VG, Ortiz JV, Foresman JB, Coslowski J, Stefanov BB, Nanayakkara A, Challacombe M, Peng CY, Ayala PY, Chen W, Wong MW, Andress JL, Replogle ES, Gomperts R, Martin RL, Fox DJ, Binkley JS, Defress DJ, Baker J, Stewart JP, Head-Gordon M, Gonzalez C, Pople JA. Guasian 98 (Revision D1), Gaussian Inc., Pittsburgh, PA, 1998.

[51] Kay HF, Wellard HJ, Vousden P. Atomic positions and optical properties of barium titanate. Nature. 1949;163:636–637. DOI: 10.1038/163636a0.

[52] MacLean DA, Ng HN, Greedan JE. Crystal structures and crystal chemistry of the $ReTiO_3$ perovskites. Re = La, Nd, Sm, Gd, Y. Journal of Solid State Chemistry. 1979;30:35–44. ISSN: 0022-4596.

[53] Gerloch M, Contable EC. Transition Metal Chemistry. Weinheim: VCH; 1994. ISBN: 978-3527292196.